

## Simulation of CO<sub>2</sub> variations at Chinese background atmospheric monitoring stations between 2000 and 2009: Applying a CarbonTracker model

CHENG YanLi<sup>1</sup>, AN XingQin<sup>1\*</sup>, YUN FangHua<sup>2</sup>, ZHOU LingXi<sup>1\*</sup>, LIU LiXin<sup>1</sup>,  
FANG ShuangXi<sup>1</sup> & XU Lin<sup>1</sup>

<sup>1</sup> Key Laboratory for Atmospheric Chemistry of China Meteorological Administration, Research Institute of Atmospheric Composition of Chinese Academy of Meteorological Sciences, Beijing 100081, China;

<sup>2</sup> School of Environmental Science and Engineering, Nanjing University of Information Science & Technology, Nanjing 210044, China

Received January 25, 2013; accepted April 22, 2013; published online June 6, 2013

We carried out a downscaling treatment over China using the CarbonTracker numerical model, which was applied using double grid nesting technology ( $3^\circ \times 2^\circ$  over the whole globe,  $1^\circ \times 1^\circ$  over China), simulating and analyzing atmospheric CO<sub>2</sub> concentrations over 10 recent years (2000–2009). The simulation results agreed very well with observed data from four background atmospheric monitoring stations in China (The periods for which the simulation results and observed values be compared were January 2000 to December 2009 for the WLG station and June 2006 to December 2009 for the SDZ, LFS, and LAN stations), giving correlation coefficients of  $>0.7$ . The high-resolution simulation data correlated slightly better than the low resolution simulation data with the observed data for three of the regions' atmospheric background stations. Further analysis of the annual, seasonal CO<sub>2</sub> concentration variations at the background stations showed that the CO<sub>2</sub> concentration increased each year over the study period, with an average annual increase of more than 5%, and annual increases of more than 7% at the Shangdianzi and Lin'an stations. Seasonal CO<sub>2</sub> variations were greater at the Longfengshan station than at the Shangdianzi or Lin'an stations. However, the CO<sub>2</sub> concentrations were higher at the Shangdianzi and Lin'an stations because they are greatly affected by human activities in the Jingjinji and Changjiang Delta economic zones. Spatial distribution in CO<sub>2</sub> concentrations and fluxes were higher in eastern than in western China.

**CarbonTracker model, numerical simulation, CO<sub>2</sub>, background atmospheric monitoring station, concentration, flux**

**Citation:** Cheng Y L, An X Q, Yun F H, et al. Simulation of CO<sub>2</sub> variations at Chinese background atmospheric monitoring stations between 2000 and 2009: Applying a CarbonTracker model. *Chin Sci Bull*, 2013, 58: 3986–3993, doi: 10.1007/s11434-013-5895-y

CO<sub>2</sub> is a greenhouse gas with a long atmospheric lifetime, and increases in its concentration will lead to increases in infrared radiation absorption by the atmosphere, and, therefore, direct radiative forcing. The fourth assessment report of the Intergovernmental Panel on Climate Change (IPCC) indicated that CO<sub>2</sub> concentrations in the atmosphere have increased from about 280  $\mu\text{mol/mol}$  before the Industrial Revolution to 379  $\mu\text{mol/mol}$  in 2005 [1]. The radiative forcing generated by the increase in atmospheric CO<sub>2</sub> con-

centrations since 1750 has been  $1.66 \pm 0.17 \text{ W/m}^2$ , which accounts for approximately 63% of the radiative forcing ( $2.30 \pm 0.23 \text{ W/m}^2$ ) generated by all long-lived greenhouse gases (CO<sub>2</sub>, CH<sub>4</sub>, N<sub>2</sub>O, and halogenated hydrocarbons). CO<sub>2</sub> radiative forcing increased by nearly 20% between 1995 and 2005; the biggest change within a decade in the last 200 years. Global warming caused by CO<sub>2</sub>, which is the dominant greenhouse gas, is therefore increasingly caused by human activities.

The observation and study of atmospheric greenhouse gases started relatively late in China. Several greenhouse

\*Corresponding authors (email: anxq@cma.cma.gov.cn; zhoulx@cma.cma.gov.cn)

gas observation stations were established from the 1980s in different regions of China, for different specific purposes [2–4]. For example, background atmospheric composition stations were established at Waliguan/Qinhai, Shangdianzi/Beijing, Lin'an/Zhejiang, Longfengshan/Heilongjiang, Xianggelila/Yunnan, Jinsha/Hubei, and Akedala/Xinjiang by the China Meteorological Administration (CMA) to observe CO<sub>2</sub> variations in the atmosphere [2,4–7]. Of these stations, the Mount Waliguan Global Atmosphere Watch Baseline Observation (WLG), the Shangdianzi station (SDZ), the Lin'an station (LAN), and the Longfengshan station (LFS) have been selected for the World Meteorological Organization's Global Atmosphere Watch network [8].

The CMA has participated in WMO round-robin reference gas inter-comparison since 1995, and has taken an active part in a series of activities organized by the World Data Center for Greenhouse Gases, the Quality Assurance – Scientific Activities Center, and the World Calibration Center. It has also regularly submitted China National Reports of greenhouse gas observations at the background stations [5]. However, the limited spatial coverage of the current surface observation system is not adequate for studying regional and global CO<sub>2</sub> concentration distributions.

Numerical simulation is an effective way of studying trace components variations in the atmosphere and their climatic effects, and can describe the relationship between variations in CO<sub>2</sub> sources and atmospheric CO<sub>2</sub> concentration, and give better spatial coverage for a long time series over a wide area. A combination of actual observations and simulation results is the best way of studying the CO<sub>2</sub> distribution and variations in the atmosphere and the source mechanisms. CarbonTracker (CT) is an atmospheric retrieval model based on the TM5 (Tracer Model, Version 5) atmospheric transmission model, developed by the National Oceanic and Atmospheric Administration Earth System Research Laboratory Global Monitoring Division (NOAA/ESRL/GMD)(<http://www.esrl.noaa.gov/gmd/ccgg/carbontracker>), which combines the atmospheric transmission model and the Kalman filter method to estimate changes in CO<sub>2</sub> absorption and emission at the earth's surface with time [9,10]. The CO<sub>2</sub> source is traced by comparison with global observations. The model is currently applied to North America and Europe.

Here, we verify the applicability of the CT model to China and present preliminary CO<sub>2</sub> concentration and flux simulation results for representative regions of China over 10 years, 2000–2009. We will also introduce CO<sub>2</sub> source and sink simulation results and predictions of future CO<sub>2</sub> concentration tendencies in another article, aiming at fully understanding the greenhouse gas concentrations and variations in China, so that the dynamics of the source variations can be understood, and so that China can make informed decisions in internal and international climate change policies.

## 1 CT model introduction and setting simulation parameters

### 1.1 CT model

The CT model uses the “top-down” method and combines an atmospheric retrieval model with ground-based observations, and other data, to establish a linear relationship between observed data and CO<sub>2</sub> sources for the real-time retrieval of CO<sub>2</sub> sources. The model has seven parts: a biosphere module that provides the terrestrial ecosystem source flux; a marine module that provides the air–sea flux; a fire module that estimates fire sources; a fossil fuel module that estimates emissions from fossil fuel combustion; TM5 model; observed data; and a Kalman filter data assimilation system. The biosphere, marine, fire, and fossil fuel combustion modules provide the initial CO<sub>2</sub> source fluxes for CT model. The TM5 atmospheric chemical transmission model is used to acquire the CO<sub>2</sub> concentration flux and other atmospheric conditions, and the data assimilation system corrects the optimized simulated CO<sub>2</sub> source flux with the Kalman filter method according to the observed data. The CT model can estimate the amount of carbon released and absorbed by natural sources (such as the biosphere, oceans, fire) and human activities (such as fossil fuel combustion), distinguishing between the natural carbon cycle and carbon emission variations caused by human activities. The CT model consists of two runs: an inverse run using 150 ensemble members, and a forward run that follows the inverse run. The inverse run determines the optimized flux parameters, but does nothing else, and the forward run is used to get all of the required output from the model (gridded fluxes, final simulated CO<sub>2</sub> values, and high-resolution mole fractions at specific sites).

### 1.2 Data sources of priori source, meteorological field, and data assimilation

The biosphere CO<sub>2</sub> flux was provided by a biosphere model (the Carnegie-Ames Stanford Approach; <http://geo.arc.nasa.gov/sge/casa/index4.html>). CO<sub>2</sub> absorbed by the ocean was calculated from the air–sea partial pressure difference [11,12]. CO<sub>2</sub> released by fire was obtained from the Global Fire Emission Database version 2 (<http://ess1.ess.uci.edu/~jranders/data/GFED2>) [13]. Emissions from fossil fuel combustion were taken from the United States Department of Energy Carbon Dioxide Information Analysis Center data on carbon dioxide discharged from global average total fossil fuel combustion ([http://cdiac.ornl.gov/trends/emis/meth\\_reg.html](http://cdiac.ornl.gov/trends/emis/meth_reg.html)) [14]. Data for the meteorological fields that drive the CT model were from the European Centre for Medium-Range Weather Forecasts (ECMWF) (<http://www.ecmwf.int/research/ifsdocs/CY28r1/index.html>). The global 3° × 2° data products from the ECMWF provided the global 3° × 2° meteorological field resolution in the CT model

directly. The  $1^\circ \times 1^\circ$  meteorological data in the Asian region were obtained from the initial ECMWF data using the same handling method as for the global  $3^\circ \times 2^\circ$  field but downscaling the simulation to the China region. The data assimilation system observational data mainly came from observed data from global and regional aerial surveys, ground-based observations, and NOAA ESRL laboratory high-tower data. The model results are from the forward run without using observed data.

### 1.3 Simulation setup

The CT model is based on the TM5 model, using global two-way grid nesting technology, nesting the regional grid in the global coarse resolution grid. The study is focused on the Chinese region, so the model is designed using a global  $3^\circ \times 2^\circ$  grid and a  $1^\circ \times 1^\circ$  grid in the Asian region. Figure 1 shows the simulation region and the nested region, D1 (global) having a resolution of  $3^\circ \times 2^\circ$  and D2 (Asian) having a resolution of  $1^\circ \times 1^\circ$ .

## 2 Verification of the CT simulation results

Because the priori source data for the CT model are at the global scale, the reliability of the simulation results for the Chinese region was verified by comparing them with observed values. Continuous  $\text{CO}_2$  observations in China are mainly available from the WLG, SDZ, LFS, and LAN stations. We compared the CT model simulation results with the observational  $\text{CO}_2$  data from these stations to verify the reliability of the simulation results.

### 2.1 Observation stations and observed data

The four background atmospheric measurement stations selected for the study are located in different ecoclimatic regions in China [6] and are reasonably representative of the region. The observed data are the continuous flask sampling

analysis results from each of the stations, which were obtained from identical sampling, analysis, and data processing methods at each station, and are comparable with other international datasets [15]. Flask sampling started at the WLG station in 1990, and samples obtained before 2006 were sent to the NOAA/ESRL laboratory for analysis. Four flask sampling series were conducted after 2006, two of which were sent to the NOAA/ESRL for analysis, the other two being analyzed by the China Meteorological Administration. The results for the 2006–2009 samples showed that the two laboratories gave very similar results ( $R^2 = 0.9669$ ,  $n = 318$ ) (Figure 2). The flask sampling at the other three background stations started in June 2006. Therefore, the periods for which the simulation results and observed values can be compared were January 2000 to December 2009 for the WLG station (because of the long flask sampling and analysis data time sequence from the NOAA/ESRL laboratory and because the results were consistent with the domestic laboratory results; the NOAA/ESRL analysis results, available at [ftp://ftp.cmdl.noaa.gov/ccg/co2/flask/event/co2\\_wlg\\_surface-flask\\_1\\_ccgg\\_event.txt](ftp://ftp.cmdl.noaa.gov/ccg/co2/flask/event/co2_wlg_surface-flask_1_ccgg_event.txt), were selected for comparison) and June 2006 to December 2009 for the SDZ, LFS, and LAN stations (the observed data being the results of the analysis by the China Meteorological Administration).

The simulation results may be different from the observed results because the simulation results are given for a grid and the model output is the numerical value for the grid point where the observation station is located, which is slightly different from the actual station location. The  $1^\circ \times 1^\circ$  and  $3^\circ \times 2^\circ$  grid parameters for the observation stations are listed in Table 1.

### 2.2 Model verification

We compared the simulation results for the two resolutions ( $1^\circ \times 1^\circ$  and  $3^\circ \times 2^\circ$ ) at each station with the observed values to verify the reliability of the simulation results and to

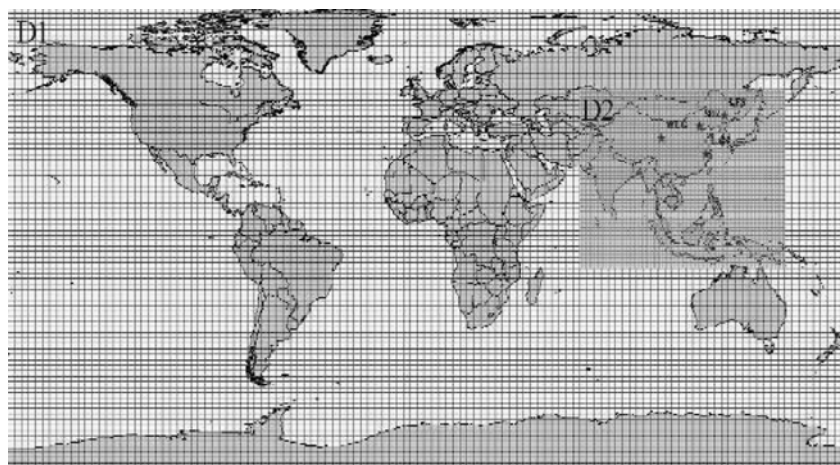


**Figure 1** The two-way nesting grid used in this study.

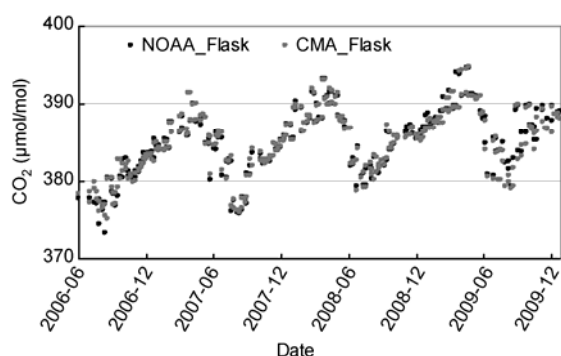


**Figure 2** CO<sub>2</sub> flask sampling results from the NOAA/ESRL and CMA analyses.

assess the influence of the resolution on the simulation results. The results are shown in Figure 3. The simulation results for all of the stations fitted the measured data well (Figure 3(a), (c), (e) and (g)). Linear regression analysis of the simulation results at the two resolutions with the measured data (Figure 3(b), (d), (f) and (h)) showed that the SDZ station had the best correlation (with an  $R$  greater than 0.9), the LFS and WLG stations had the next best correlations (each with an  $R$  of approximately 0.85), and the LAN station had the poorest correlation (but still with an  $R$  greater than 0.7). It can be seen that, except for at the WLG station, the correlation between the  $1^\circ \times 1^\circ$  simulation results and the observed data was better than between the  $3^\circ \times 2^\circ$  simulation results and the observed data, indicating that downscaling the model gives results much closer to the values measured at the regional stations.

### 3 Results and discussion

The CT model can be seen to effectively reflect the observed data, from comparing the simulation results and the actual measurements. Further analyses of the simulation results, to investigate the long-term (2000–2009) variations in CO<sub>2</sub> concentrations in different areas of China are shown below, and, in particular, the results was trace back to changes trend in CO<sub>2</sub> concentrations at the regions background atmospheric stations (2000–2006) (i.e. flask sampling at the SDZ, LFS, and LAN background atmospheric stations started in June 2006).

#### 3.1 Annual CO<sub>2</sub> concentration variations

Table 2 shows the annual mean CO<sub>2</sub> concentrations from the  $1^\circ \times 1^\circ$  resolution simulation results for the four background atmospheric monitoring stations from 2000 to 2009. The annual mean CO<sub>2</sub> concentration at each station increased every year.

Figure 4 shows the monthly mean CO<sub>2</sub> concentration simulation results, which rise, in agreement with the daily mean CO<sub>2</sub> concentration trend (Here is no display), from 2000 to 2009. The SDZ and LAN stations showed relatively sharp rises, increasing by 27.89  $\mu\text{mol/mol}$  and 26.75  $\mu\text{mol/mol}$  (equivalent to increases of 7.31% and 7.03%), respectively, over the 10 years studied. The changes at the SDZ and LAN stations are caused by regional human activities. In contrast, the LFS and WLG stations showed relatively slow increases in CO<sub>2</sub> concentrations, by 20.56  $\mu\text{mol/mol}$  and 20.27  $\mu\text{mol/mol}$  (equivalent to increases of 5.44% and 5.46%), respectively, over the 10 years studied, possibly because CO<sub>2</sub> concentrations at these stations are mainly affected by the regional ecological systems. The background atmospheric CO<sub>2</sub> concentration at the WLG station was relatively low and changed smoothly, similar to the global average atmospheric CO<sub>2</sub> concentration trend. The global average atmospheric CO<sub>2</sub> concentration in 2009 was 386.8  $\mu\text{mol/mol}$  [16]. The validation results showed that the CT model predicted slightly higher average rates of CO<sub>2</sub> concentration increases for the four stations studied in China than has been reported for the globe for the same period [16] or from satellite observations for China between 2003 and 2008 [17].

#### 3.2 Seasonal CO<sub>2</sub> concentration variations

Figure 5 shows clear seasonal variations in the  $1^\circ \times 1^\circ$  resolution CO<sub>2</sub> concentration simulation results for each of the background station grids in the 10 years studied (2000–2009). Seasonal variations in the background CO<sub>2</sub> concentrations are caused by CO<sub>2</sub> uptake and release processes in the geo-ecosystem, CO<sub>2</sub> emission from human activities, CO<sub>2</sub> uptake by the ocean, and some specific events [18,19]. The atmospheric CO<sub>2</sub> concentration reached a clear minimum every summer and a maximum mainly in the spring or winter, which fits the trend seen in the observed data [6,20]. The CO<sub>2</sub> concentration at the WLG station showed typical

**Table 1** Locations of the stations and the grid points for the stations in the model

Station	Station		$1^\circ \times 1^\circ$ grid		$3^\circ \times 2^\circ$ grid	
	Longitude ( $^\circ$ )	Latitude ( $^\circ$ )	Longitude ( $^\circ$ )	Latitude ( $^\circ$ )	Longitude ( $^\circ$ )	Latitude ( $^\circ$ )
WLG	100.90	36.29	100.5	36.5	100.5	37.0
SDZ	117.07	40.39	117.5	40.5	118.5	41.0
LFS	127.60	44.73	127.5	44.5	127.5	45.0
LAN	119.73	30.30	119.5	30.5	118.5	31.0

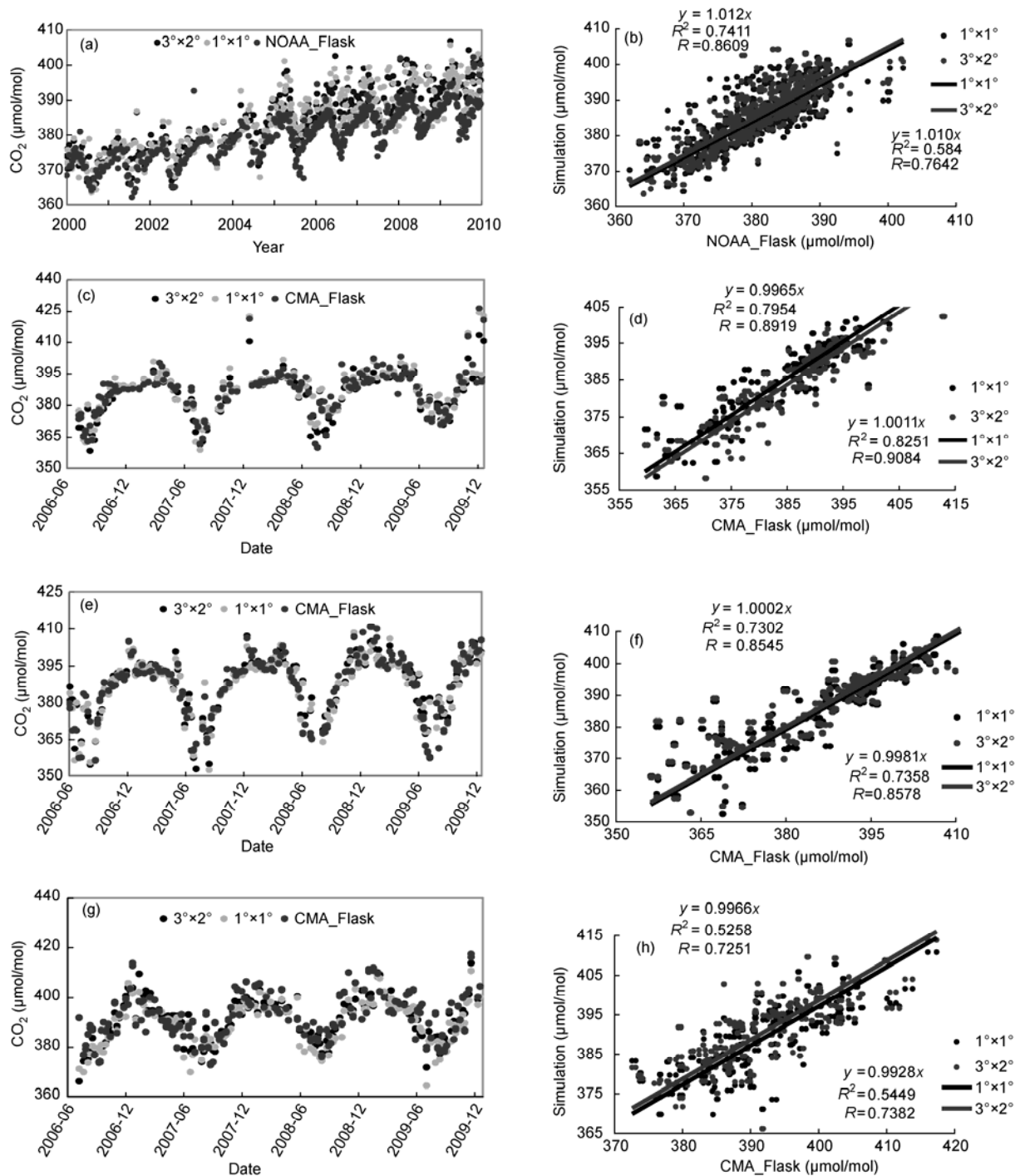


**Figure 3** Comparison of  $3^{\circ} \times 2^{\circ}$  and  $1^{\circ} \times 1^{\circ}$  simulation values with observed CO<sub>2</sub> concentrations from the flask sampling in four stations ((a) WLG; (c) SDZ; (e) LFS; (g) LAN) and linear regression analysis of the simulation results at the two model resolutions with the measured data ((b) WLG; (d) SDZ; (f) LFS; (h) LAN).

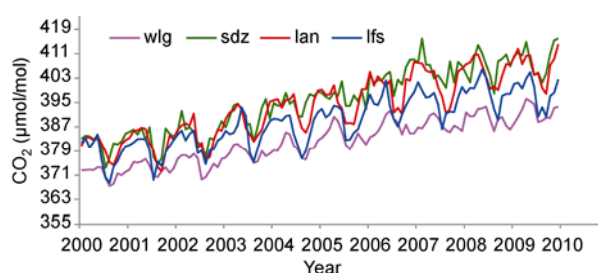
spring maxima and summer minima, with a range of 7.81 μmol/mol. This result agrees with the long-term observation data from the WLG station, and is caused by the strong influence of the biosphere on the atmosphere.

The seasonal variation in the atmospheric CO<sub>2</sub> concentration was significant at the LFS station (with a seasonal

fluctuation of 14.71 μmol/mol), and the CO<sub>2</sub> concentration here is mainly affected by the ecological system rather than anthropogenic emission. In contrast, the SDZ and LAN station data reflect CO<sub>2</sub> concentrations in more developed areas, mainly being affected by anthropogenic emissions. Seasonal anthropogenic emission variations in these developed areas

**Table 2** Annual mean CO<sub>2</sub> concentrations at the four background atmospheric monitoring stations for 2000–2009 (unit:  $\mu\text{mol/mol}$ )

Year	LAN	LFS	SDZ	WLG
2000	380.51	377.94	381.45	371.54
2001	381.69	379.33	382.95	373.48
2002	384.15	381.71	384.73	375.04
2003	389.23	385.04	390.26	378.32
2004	393.35	386.34	395.06	380.44
2005	394.97	389.52	396.72	384.25
2006	400.25	394.65	403.72	387.03
2007	401.86	395.40	406.02	387.70
2008	405.42	398.46	407.08	390.06
2009	407.26	398.51	409.35	391.81
Total increase in 10 a	26.75	20.56	27.89	20.27
Percentage increase in 10 a (%)	7.03	5.44	7.31	5.46

**Figure 4** Monthly mean atmospheric CO<sub>2</sub> concentrations at each background atmospheric station from 2000 to 2009.

are not distinctive, so the seasonal atmospheric CO<sub>2</sub> concentration ranges are lower at the SDZ and LAN stations than at the LFS station. However, the Jingjinji and Changjiang Delta economic zones, which are near the SDZ and LAN stations, are industrialized and urbanized areas that have large populations and high CO<sub>2</sub> emissions caused by

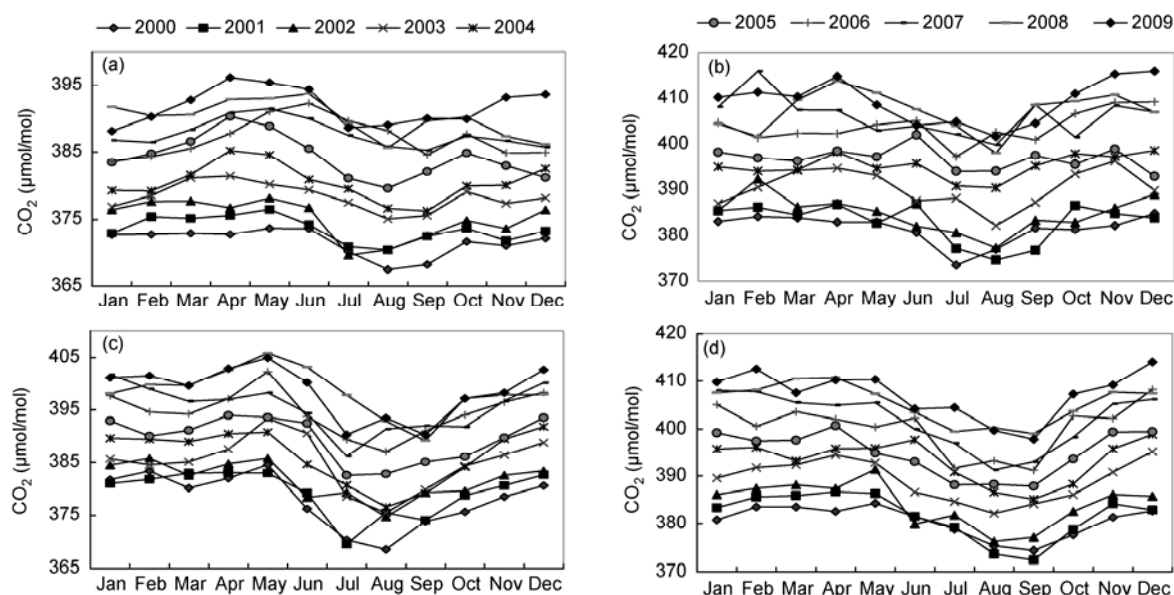
human activities, so the CO<sub>2</sub> concentrations are higher at the SDZ and LAN stations than at the LFS station.

### 3.3 CO<sub>2</sub> concentration and net flux variations

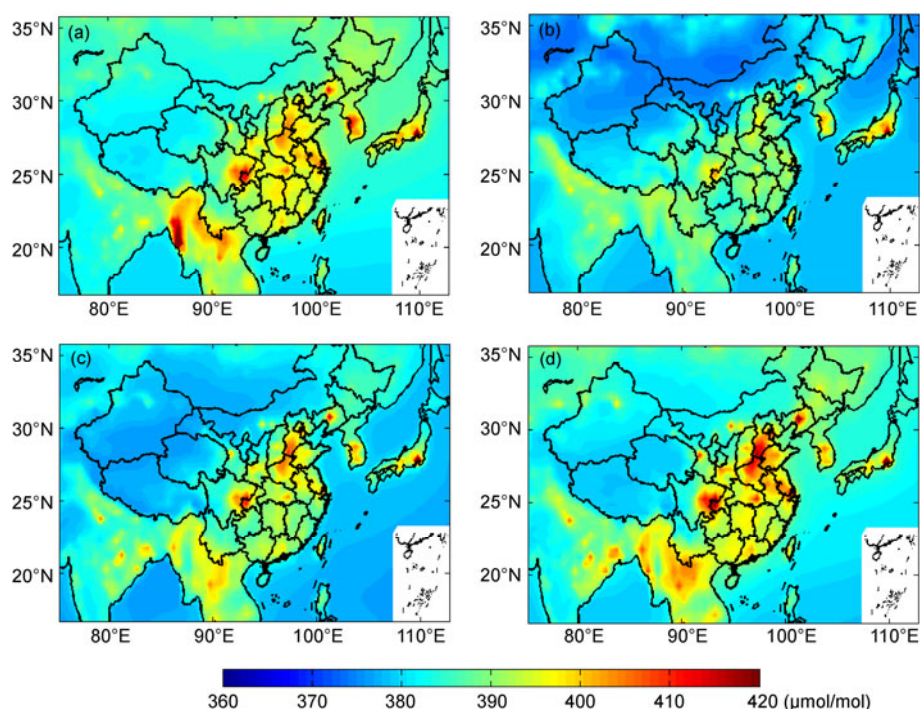
Figures 6 and 7 show averaged seasonal variations in the spatial distribution of CO<sub>2</sub> concentrations and fluxes over China for 2000–2009 (spring = March–May, summer = June–August, autumn = September–November, winter = December–February of the next year).

The atmospheric CO<sub>2</sub> concentrations over China were generally higher in the east than in the west. Specifically, high CO<sub>2</sub> concentration, of up to 420  $\mu\text{mol/mol}$ , was found in eastern Sichuan, southwestern Chongqing, southern Shanghai, Jiangsu and Hebei, northern Henan, Beijing, Tianjin and the northeast. Atmospheric CO<sub>2</sub> concentrations were around 380–390  $\mu\text{mol/mol}$  in northwestern China and Tibet. These differences could be explained by the differences in vegetation in the eastern and western regions, but China has been developing economically at a very high rate, and uneven regional economic development will have led to regional differences in atmospheric CO<sub>2</sub> concentrations. The CO<sub>2</sub> concentrations were different in different seasons, and the CO<sub>2</sub> concentration was lower overall in the summer than in the other seasons.

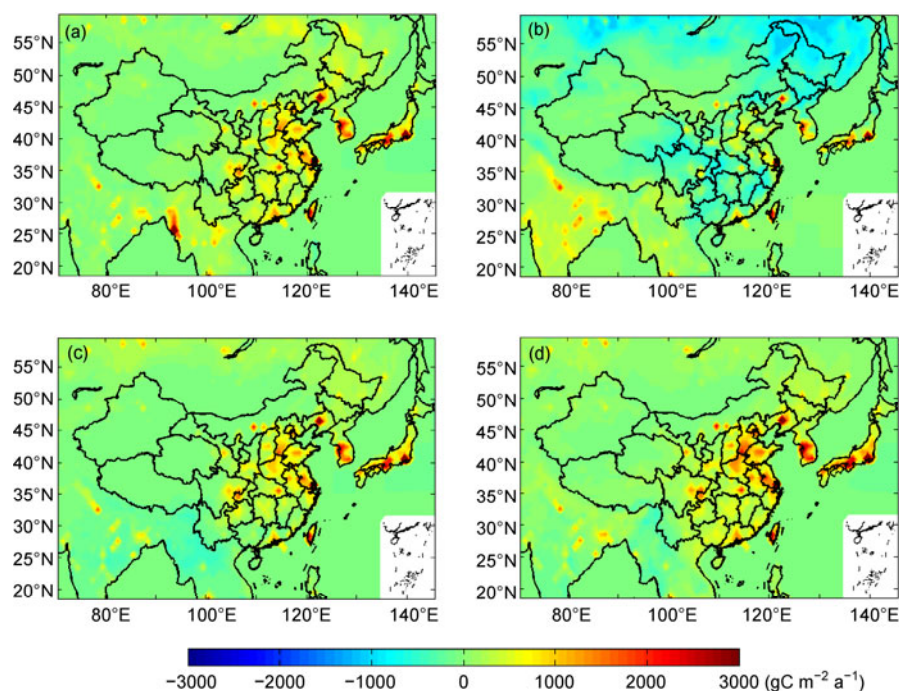
The CO<sub>2</sub> flux simulation results show that the average net CO<sub>2</sub> flux was positive between 2000 and 2009, meaning that China was a net carbon source (except in the summer). The spatial distribution of the CO<sub>2</sub> fluxes was similar to the distribution of the CO<sub>2</sub> concentrations, and the distribution characteristics were consistent with the CO<sub>2</sub> emission sources that have been reported [21]; that is, gradually decreasing from east to west. Tibet, western Sichuan, northern Inner Mongolia, and southern Xinjiang CO<sub>2</sub> emission fluxes were very low, and almost zero.

**Figure 5** Seasonal atmospheric CO<sub>2</sub> concentration means in different years at the four stations. (a) WLG; (b) SDZ; (c) LFS; (d) LAN.





**Figure 6** (Color online) Averaged seasonal variations in the spatial distribution of CO<sub>2</sub> concentrations over China between 2000 and 2009. (a) Spring; (b) summer; (c) autumn; (d) winter.



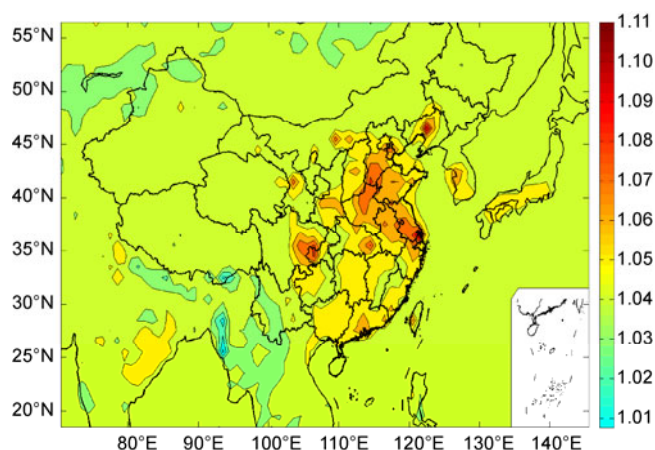
**Figure 7** (Color online) Averaged seasonal variations in the spatial distribution of CO<sub>2</sub> fluxes over China between 2000 and 2009. (a) Spring; (b) summer; (c) autumn; (d) winter.

Figure 8 shows the spatial distribution of the growth rate of the CO<sub>2</sub> concentrations, comparing 2008 with 2001. The growth rate has obvious regional characteristics, with the most significant areas of increasing concentrations being Jingjinji, the Changjiang Delta, the Pearl River Delta, eastern Sichuan, and Chongqing. This distribution is consistent with the four main economic zones and the high-speed

economic development zones, which have high levels of anthropogenic emissions.

## 4 Conclusions

(1) We downscaled the CO<sub>2</sub> concentration simulation for



**Figure 8** (Color online) Spatial distribution of the growth rate of CO<sub>2</sub> concentrations (i.e. the ratio of the CO<sub>2</sub> concentration in 2008 to the CO<sub>2</sub> concentration in 2001).

China using a nested grid in a CT model, and found good agreement between the simulation results and the observed data by comparing the long-term CO<sub>2</sub> concentrations observed at four background atmospheric monitoring stations in China with the CT model simulation results in the grids containing those stations. We also found that the high-resolution simulation results ( $1^{\circ} \times 1^{\circ}$ ) were more accurate than the low resolution simulation results ( $3^{\circ} \times 2^{\circ}$ ).

(2) The CT model simulation results showed that the CO<sub>2</sub> concentrations rose year-on-year for the 10 years studied at the four background atmospheric monitoring stations. Increases in the CO<sub>2</sub> concentrations were higher at the SDZ and LAN stations than at the WLG and the LFS stations. Seasonal CO<sub>2</sub> concentration variations were higher at the LFS station than at the SDZ and LAN stations, which reflects, to some extent, the background atmospheric CO<sub>2</sub> concentrations in the more developed regions where the SDZ and LAN stations are located. The LFS station represents undeveloped areas that are relatively little affected by anthropogenic emissions. Seasonal fluctuations fitted the trend found in the observed data.

(3) The CT simulation results showed that the CO<sub>2</sub> concentrations and fluxes were higher in the east than in the west of China, which matches the level of economic development, population density, and CO<sub>2</sub> emission source distributions.

*This work was supported by the National Basic Research Program of China (2010CB950601), the International S & T Cooperation Program MOST (2011DFA21090), and the National Natural Science Foundation of China (41175116). We appreciate the help of NOAA/ESRL/GMD in providing the CarbonTracker model and technical support (Jacobson and others). We thank the main developers of TM5 (Krol, Segers, and others) and all the observer staff at the Waliguan Atmospheric Background Station, the Shangdianzi Station, the Lin'an Station, and the Longfeng Mountain Station for their commitment in preparing and analyzing samples.*

**Open Access** This article is distributed under the terms of the Creative Commons Attribution License which permits any use, distribution, and reproduction in any medium, provided the original author(s) and source are credited.

- 1 IPCC. Climate Change 2007: The Physical Science Basis. IPCC Secretariat, 2007
- 2 Wen Y P, Tang J, Shao Z Q, et al. A study of atmospheric CO<sub>2</sub> concentration variations and emission from the soil surface at Mt. Waliguan (in Chinese). *Q J Appl Meteorol*, 1997, 8: 129–136
- 3 Wang M X, Liu W W, Rasmussen R A, et al. Long-term trend and seasonal cycle of atmospheric methane. *Chin Sci Bull*, 1990, 35: 213–216
- 4 Wang G C, Wen Y P, Kong Q X, et al. CO<sub>2</sub> background concentration in the atmosphere over the Chinese mainland. *Chin Sci Bull*, 2002, 47: 1217–1220
- 5 Zhou L X, Zhou X J, Zhang X C, et al. Progress in the study of background greenhouse gases at Waliguan observatory (in Chinese). *Acta Meteorol Sin*, 2007, 65: 458–468
- 6 Liu L X, Zhou L X, Zhang X C, et al. The characteristics of atmospheric CO<sub>2</sub> concentration variation of four national background stations in China. *Sci China Ser D-Earth Sci*, 2009, 52: 1857–1863
- 7 Zhao Y C, Wen Y P, De Li Ge Le, et al. Change characteristics of atmospheric CO<sub>2</sub> background concentration in Waliguan, Qinghai (in Chinese). *Chin Environ Sci*, 2006, 26: 1–5
- 8 Zhou L X, Liu L X, Zhang X C, et al. Preliminary results on network observation of greenhouse gases at China GAW stations (in Chinese). *J Appl Meteorol Sci*, 2008, 19: 641–645
- 9 Peters W, Jacobson A R, Sweeney C, et al. An atmospheric perspective on North American carbon dioxide exchange: CarbonTracker. *Proc Natl Acad Sci USA*, 2007, 104: 18925–18930
- 10 Krol M, Houweling S, Bregman B, et al. The two-way nested global chemistry-transport zoom model TM5: Algorithm and applications. *Atmos Chem Phys*, 2005, 5: 417–432
- 11 Gloor M, Gruber N, Sarmiento J, et al. A first estimate of present and preindustrial air-sea CO<sub>2</sub> flux patterns based on ocean interior carbon measurements and models. *Geophys Res Lett*, 2003, 30: 10.1029/2002GL015594
- 12 Gruber N, Sarmiento J L, Stocker T F. An improved method for detecting anthropogenic CO<sub>2</sub> in the oceans. *Glob Biogeochem Cycle*, 1996, 10: 809–837
- 13 van der Werf G R, Randerson J T, Giglio L, et al. Interannual variability in global biomass burning emissions from 1997 to 2004. *Atmos Chem Phys*, 2006, 6: 3423–3441
- 14 Marland G. Uncertainties in accounting for CO<sub>2</sub> from fossil fuels. *J Ind Ecol*, 2008, 12: 136–139
- 15 Zhang X C, Cai Y X, Wen Y P, et al. Study of Atmospheric Carbon Dioxide Calibration and Flask Sample Analysis System (in Chinese). *Meteorol Sci Technol*, 2005, 33: 538–547
- 16 World Meteorological Organization. Greenhouse Gas Bulletin: The State of Greenhouse Gases in the Atmosphere Using Global Observations through 2009. 2010
- 17 Bai W G, Zhang X Y, Zhang P. Temporal and spatial distribution of tropospheric CO<sub>2</sub> over China based on satellite observations. *Chin Sci Bull*, 2010, 55: 3612–3618
- 18 Dettinger M D, Ghil M. Seasonal and interannual variations of atmospheric CO<sub>2</sub> and climate. *Tellus*, 1998, 50B: 1–24
- 19 Wittenberg U, Heiman M, Esser G, et al. On the influence of biomass burning on the seasonal CO<sub>2</sub> signal as observed at monitoring stations. *Glob Biogeochem Cycle*, 1998, 12: 531–544
- 20 Pu J J, Xu H H, Kang L L, et al. Characteristics of atmospheric CO<sub>2</sub> concentration and variation of carbon source & sink at Lin'an regional background station (in Chinese). *Environ Sci*, 2011, 32: 2221–2225
- 21 Bai B, Li X C, Liu Y F, et al. Preliminary study on CO<sub>2</sub> industrial point sources and their distribution in China (in Chinese). *Chin J Rock Mech Eng*, 2006, 25: 2918–2923